Synthesis of Metal and Metal Oxide Nanowire and Nanotube Arrays within a Mesoporous Silica Template

Timothy A. Crowley,[†] Kirk J. Ziegler,[†] Daniel M. Lyons,[†] Donats Erts,[‡] Håkan Olin,[§] Michael A. Morris,[†] and Justin D. Holmes*[,†]

Department of Chemistry, Materials Section and Supercritical Fluid Centre, University College Cork, Cork, Ireland, Institute of Chemical Physics, University of Latvia, LV-1586 Riga, Latvia, and Physics and Engineering Physics, Chalmers University of Technology, SE-412 96 Göteborg, Sweden

Received March 10, 2003. Revised Manuscript Received June 17, 2003

Metallic nanowires of cobalt, copper, and iron oxide magnetite (Fe_3O_4) have been synthesized within the pores of mesoporous silica using a supercritical fluid inclusion technique. The mesoporous matrix provides a means of producing a high density of stable, hexagonally ordered arrays of highly crystalline nanowires. The formation of the metal and metal oxide nanowires within the silica mesopores was confirmed by transmission electron microscopy (TEM), N_2 adsorption experiments, and powder X-ray diffraction (PXRD). The mechanism of nanowire formation within the mesopores appears to occur through the initial binding and coating of the pore walls with the metal atoms to form tubelike structures within the mesoporous template. The thickness of these tubes subsequently increases with further metal deposition until nanowires are formed. Additionally, the crystal structure of the cobalt nanowires formed within the mesoporous template can be readily changed by manipulating the density of the supercritical fluid phase.

Introduction

Highly ordered arrays of metallic nanowires are expected to play an essential role as materials for interconnects and high-density magnetic storage devices because of their unique electrical and magnetic properties.[1,2] For example, Lederman and others have previously suggested that a patterned magnetic nanowire array could be used as an ultra-high-density recording medium with recording densities on the order of 100 Gbit/in^2.[3−5] Magnetite (Fe_3O_4) also has potential uses in spin electronic devices due to its intrinsic half-metallic ferrimagnetic nature.[6]

One promising technique for the integration of nanowires into well-defined architectures is their deposition into ordered templates. Arrays of cobalt, copper, and iron nanowires have previously been synthesized by electrodeposition in porous templates such as anodic aluminum oxide (AAO),[3,7−13] polycarbonate track membranes,[14−17] and diblock copolymers.[18,19] While these template methods have some applications, it is difficult to form high densities of ordered nanowires that exhibit quantum confinement effects required for future nanoscale devices. Hexagonal mesoporous silicas, however, have uniform cylindrical pores between 2 and 30 nm in diameter, making them ideally suited as template architectures for nanometer-scale metallic wire arrays. Mesoporous solids have previously served as templates

* To whom correspondence should be addressed. Telephone: +353 (0)21 4903608. Fax: +353 (0) 21 4274097. E-mail: j.holmes@ucc.ie.
† University College Cork.
‡ University of Latvia.
§ Chalmers University of Technology.

(1) White, T. W.; New, R. M. H.; Pease, R. F. W. *IEEE Trans. Magn.* **1996**, *33*, 990.
(2) Routkevitch, D.; Tager, A. A.; Haruyama, J.; Almawlawi, D.; Moscovitz, M.; Xu, J. M. *IEEE Trans. Electron Devices* **1996**, *31*, 1646.
(3) Lederman, M.; O'Barr, R.; Schultz, S. *Trans. Magn.* **1995**, *31*, 3793.
(4) Dinega, D. P.; Bawendi, M. G. *Angew. Chem., Int. Ed.* **1999**, *38*, 1788.
(5) Kitakami, O.; Satao, H.; Shimada, Y.; Sato, F.; Tanaka, M. *Phys. Rev. B* **1997**, *56*, 13849.
(6) van der Zaag, P. J.; Bloemen, P. J. H.; Gaines, J. M.; Wolf, R. M.; van der Heijden, P. A. A.; van de Veerdonk, R. J. M.; de Jonge, W. J. M. *J. Magn. Magn. Mater.* **2000**, *211*, 301.
(7) Metzger, R. M.; Konovalov, V. V.; Sun, M.; Xu, T.; Zangari, G.; Xu, B.; Benakli, M.; Doyle, W. D. *IEEE Trans. Magn.* **2000**, *36*, 30.
(8) Paulus, P. M.; Luis, F.; Kroll, M.; Schmid, D.; de Jongh, L. J. *J. Magn. Magn. Mater.* **2001**, *224*, 180.
(9) Zhang, X. Y.; Zhang, L. D.; Chen, W.; Meng, G. W.; Zheng, M. J.; Zhao, L. X. *Chem. Mater.* **2001**, *13*, 2511.
(10) Khan, H. R.; Petrikowski, K. *J. Magn. Magn. Mater.* **2002**, *215−216*, 526.
(11) Yang, S.; Zhu, H.; Yu, D.; Jin, Z.; Tang, S.; Du, Y. *J. Magn. Magn. Mater.* **2000**, *222*, 97.
(12) Blythe, H. J.; Fedosyuk, V. M.; Kasyutich, O. I.; Schwarzacher, W. *J. Magn. Magn. Mater.* **2000**, *208*, 251.
(13) Nielsch, K.; Wehrspohn, R. B.; Barthel, J.; Kirschner, J.; Gosele, U.; Fischer, S. F.; Kronmuller, H. *Appl. Phys. Lett.* **2001**, *79*, 1360.
(14) Heyton, G. P.; Hoon, S. R.; Farley, A. N.; Tomlinson, S. L.; Valera, M. S.; Attenborought, K.; Schwarzecher, W. *Appl. Phys.* **1997**, *30*, 1083.
(15) Scarani, V.; Doudin, B.; Ansermet, J. *J. Magn. Magn. Mater.* **1999**, *205*, 241.
(16) Dubois, S.; Beuken, J. M.; Piraux, L.; Duvail, J. L.; Fert, A.; George, J. M.; Maurice, J. L. *J. Magn. Magn. Mater.* **1997**, *165*, 30.
(17) Belliard, L.; Miltat, J.; Thiaville, A.; Dubois, S.; Duvail, J. L.; Piraux, L. *J. Magn. Magn. Mater.* **1998**, *190*, 1.
(18) Thurn-Albrecht, T.; Schotter, J.; Kastle, G. A.; Emley, N.; Shibauchi, T.; Krusin-Elbaum, L.; Guarini, K.; Black, T.; Touminen, M. T.; Russell, T. P. *Science* **2000**, *290*, 2126.
(19) Thurn-Albrecht, T.; Russell, T. P.; Steiner, U. *Nature* **2000**, *403*, 874.

10.1021/cm034139v CCC: $25.00
Published on Web 07/31/2003

for nanostructured metals deposited by such techniques as incipient wetness[20,21] and ion exchange.[22] In particular, Zhang et al.[23] reported the synthesis of copper and nickel nanowires using a multistep electroless deposition method. These techniques have met with some success, but have been unable to achieve complete filling of the pores with nanowires or nanoparticles. Recently, we reported almost complete (95%) filling of the mesoporous silica powders with silicon and germanium nanowires using a supercritical fluid (SCF) phase inclusion technique.[24−26] The high diffusivity and low viscosity of the SCF leads to substantial solvent penetration of the porous silica matrix and rapid transport of the semiconductor precursors into the mesopores where nucleation and growth of the nanowire array readily occurs. Additionally, we have recently shown that the pore diameter and, hence, nanowire width can be controlled with Angström-level precision.[27,28]

Here, we describe the adaptation of our SCF inclusion phase technique, previously used for semiconductor nanowire inclusion, to form ordered arrays of nanowires and nanotubes of cobalt, copper, and iron oxide within mesoporous silica matrixes. In this article we describe how metallic nanowire and nanotubes were synthesized using carbon dioxide (CO_2) as the fluid phase solvent rather than supercritical (sc) hexane, which was used in our prior inclusion processes.[24−26,28] CO_2 is an ideal solvent for this inclusion process as it is nontoxic, nonreactive, and relatively inexpensive. Additionally, using CO_2 rather than organic solvents helps to minimize impurities during nanowire processing.

Experimental Section

Hexagonal mesoporous silica powder was prepared by hydrolyzing tetramethoxysilane (TMOS) in the presence of a poly(ethylene oxide) (PEO)−poly(propylene oxide) (PPO) triblock copolymer surfactant, Synperonic P85 ($PEO_{26}PPO_{39}PEO_{26}$), or P123 ($PEO_{20}PPO_{69}PEO_{20}$) (Uniquema, Belgium) and HCl (0.5 M). In a typical synthesis, Synperonic P85 or P123 (1 g) was dissolved in TMOS (1.8 g, 0.0118 mol) and added to an aqueous solution of HCl (1 g, 0.5 M). Methanol generated during the reaction was removed on a rotary evaporator at 40 °C. The resulting viscous gel was left to condense at 40 °C for 1 week in a sealed flask. Calcination of the silica was undertaken in air for 24 h at 450 °C. The silica matrix was degassed prior to inclusion using the Flowprep 060 Degasser from Micrometrics. Pure, dry N_2 was passed over the heated mesoporous matrix at 200 °C to remove moisture and other contaminants.

Metal and metal oxide nanowires were synthesized within the mesoporous silica powder by degrading the appropriate organometallic precursor in supercritical carbon dioxide (sc-CO_2). Dicobalt octacarbonyl, copper(II) hexafluoroacetylacetonate hydrate, and iron dodecacarbonyl were used as precursors. Copper(II) hexafluoroacetylacetonate hydrate is known to be highly soluble in sc-CO_2[29] and has been utilized in the synthesis of copper particles[30] and thin films.[31] Iron dodecacarbonyl was stabilized with 5% methanol to prevent decomposition. Mesoporous silica powder (0.5 g) and the organometallic precursor (0−12 mmol) were added to the high-pressure reactor inside a nitrogen glovebox. The high-pressure reaction cell was attached to a 260-mL ISCO syringe pump (Lincoln, NE) via a three-way valve and then placed in a tube furnace and heated to the reaction temperature. While heating, the solvent pressure was ramped to the desired reaction pressure. Synthesis conditions were varied with temperatures ranging from 300 to 500 °C and pressures of 138−345 bar. After the temperature within the reaction cell was achieved, the reaction proceeded for 30 min. Upon completion, the cell was cooled and the contents of the cell were washed with dry hexane.

High-resolution transmission electron microscopy (HR-TEM) was performed on a Philips CM200 Super TWIN FEG operating at 200 kV. Typically, 20 mg of sample was dispersed in 20 mL of absolute ethanol and a drop of the resultant solution was dispersed on a carbon-coated, 400-mesh, copper grid. Powder X-ray diffraction (PXRD) data was collected on a Philips PW3710 MPD diffractometer using Cu $K\alpha_1$ radiation with an anode current of 40 mA and an accelerating voltage of 40 kV. The quantitative analysis of each phase was determined by fitting the powder patterns with simulated patterns using PC-Rietveld. A Micrometrics Gemini III 2375 surface area analyzer was used to collect the Brunauer−Emmett−Teller (BET) and Barrett, Joyner, and Halenda (BJH) surface area and pore size distributions. Fourier transform infrared (FTIR) spectroscopy was measured on a Bio-Rad FTS 3000 FTIR spectrophotometer.

Results and Discussion

Figure 1a shows a TEM image of P123 mesoporous silica powder. The image displays a hexagonal array of mesopores with a pore diameter of 7 nm and a pore center-to-center distance of 10 nm. P85 mesoporous silica powders shown in Figure 1b had pore diameters of 5 nm and a pore center-to-center distance of 8.5 nm. After inclusion, a series of parallel cobalt nanowires can be seen within a P85 mesoporous silica template shown in Figure 2a. These nanowires are 5 nm in diameter and can be over 1 μm in length, resulting in aspect ratios over 200. The nanowires are separated by silica pore walls approximately 3 nm in length. Hence, nanowire

(20) Napolsky, K. S.; Eliseev, A. A.; Knotko, A. V.; Lukahsin, A. V.; Vertegel, A. A.; Tretyakov, Y. D. *Mater. Sci. Eng.* **2003**, *23*, 151.
(21) Han, Y.; Kim, J. M.; Stucky, G. D. *Chem. Mater.* **2000**, *12*, 2068.
(22) Ryoo, R.; Ko, C. H.; Kim, J. M.; Howe, R. *Catal. Lett.* **1996**, *27*, 29.
(23) Zhang, Z.; Dai, S.; Blom, D. A.; Shen, J. *Chem. Mater.* **2002**, *14*, 965.
(24) Coleman, N. R. B.; Ryan, K. M.; Spalding, T. R.; Holmes, J. D.; Morris, M. A. *Chem. Phys. Lett.* **2001**, *343*, 1.
(25) Coleman, N. R. B.; Morris, M. A.; Spalding, T. R.; Holmes, J. D. *J. Am. Chem. Soc.* **2001**, *123*, 187.
(26) Coleman, N. R. B.; O'Sullivan, N.; Ryan, K. M.; Crowley, T. A.; Morris, M. A.; Spalding, T. R.; Steytler, D. C.; Holmes, J. D. *J. Am. Chem. Soc.* **2001**, *123*, 7010.
(27) Ryan, K. M.; Coleman, N. R. B.; Lyons, D. M.; Hanrahan, J. P.; Spalding, T. R.; Morris, M. A.; Steytler, D. C.; Heenan, R. K.; Holmes, J. D. *Langmuir* **2002**, *18*, 4996.
(28) Lyons, D. M.; Ryan, K. M.; Morris, M. A.; Holmes, J. D. *Nano Lett.* **2002**, *2*, 811.
(29) Lagalante, A. F.; Hansen, B. N.; Bruno, T. J. *Inorg. Chem.* **1995**, *34*, 5781.
(30) Garriga, R.; Pessey, V.; Weill, F.; Chevalier, B.; Etourneau, J.; Cansell, F. *J. Supercrit. Fluid* **2001**, *20*, 55.
(31) Blackburn, J. M.; Long, D. P.; Cabanas, A.; Watkins, J. J. *Science* **2001**, *294*, 141.

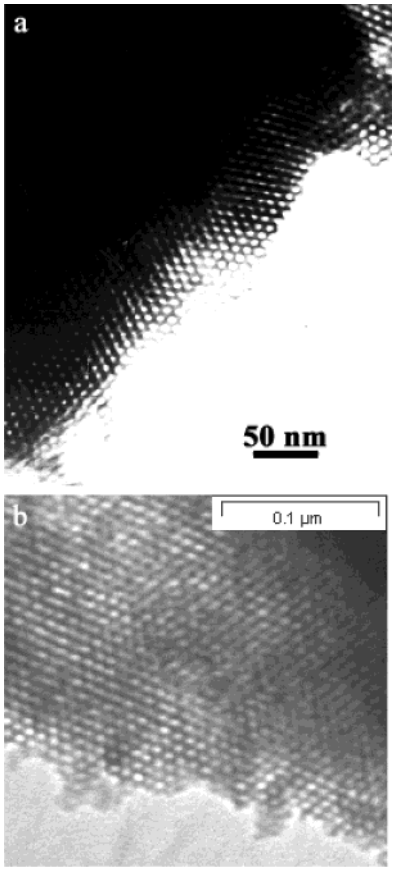

Figure 1. TEM image of calcined (a) P123 and (b) P85 mesoporous silica powder.

array densities of 10^{12} nanowires/cm^2 are achievable. The nanowires are single crystals as shown by the selected area electron diffraction pattern (inset, Figure 2a). Figure 2b shows a high-resolution TEM image of a single nanowire of Fe_3O_4 grown within a pore of P123 mesoporous silica. These nanowires are highly crystalline and exhibit a lattice spacing of 1.73 Å corresponding to the ⟨422⟩ lattice plane of magnetite.[32,33]

PXRD analysis of the iron oxide nanowires shown in Figure 2b confirmed that the nanowires were composed of Fe_3O_4, a ferrimagnetic oxide naturally occurring as the mineral magnetite (Figure 3a). Fe_3O_4 was formed preferentially to metallic iron or Fe_2O_3 due to the partially oxidizing nature of the reaction environment. Oxygen was present in the reaction mixture due to the presence of methanol, which is used to stabilize the iron dodecacarbonyl precursor; all other sources of oxygen and moisture were excluded from the reaction environment. Figure 3b shows the PXRD pattern recorded for copper nanowires grown within mesoporous P85 silica and is characteristic of cubic copper with peaks at 43.5°, 50.5°, and 74° 2θ corresponding to the ⟨111⟩, ⟨200⟩, and ⟨220⟩ planes, respectively.[32] The extremely broad peak at a 2θ angle of 20° is due to scattering from the amorphous silica framework.[26]

(32) Calculated from ICSD using POWD-12++, 1997.

(33) Note that the common morphology of magnetite crystals usually involves ⟨110⟩ faces. Explicitly, the ⟨211⟩ direction is rotated 19.5° in the the ⟨0,1,−1⟩ direction from the ⟨111⟩ direction. The image shown in Figure 1 is a representation of a ⟨211⟩ plane through a ⟨110⟩ face.

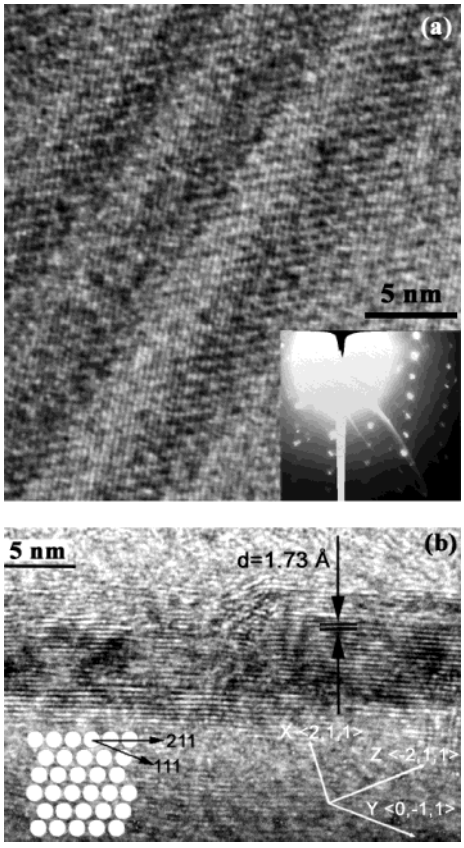

Figure 2. HRTEM image of (a) a series of parallel cobalt nanowires. The inset shows the SAED pattern of the cobalt nanowires. (b) An individual Fe_3O_4 nanowire synthesized in mesoporous silica at 450 °C and 345 bar. The *d* spacing of 1.73 Å shown is assigned to the crystal spacing of ⟨422⟩ planes. Also shown is the relationship of the equivalent ⟨211⟩ directions to a vicinal ⟨110⟩ direction and the ⟨211⟩ crystal plane projected onto the ⟨0,1,−1⟩ plane.

Cobalt is known to have three crystal structures, hexagonal close-packed (hcp), face-centered cubic (fcc), and the recently discovered and less dense metastable cubic phase (ϵ).[34] The formation of the common phases (hcp and fcc) is known to be temperature-dependent, with the fcc structure being thermodynamically preferred at temperatures above 450 °C and the hcp phase favored at lower temperatures.[4] In our SCF procedure, we have found that the formation of the ϵ-phase is not only temperature- but also pressure-mediated. At a constant pressure of 345 bar, Co nanowires prepared at temperatures below 500 °C displayed a mixture of HCP (α) and FCC (β) phases as shown in Table 1. Increasing the temperature to 500 °C at 345 bar results in the formation of only the fcc β phase. At the lower pressure of 276 bar and temperatures below 500 °C, the ϵ-phase is witnessed along with the α and β phases as seen in the PXRD pattern of Figure 3c. Increasing the synthesis temperature to 500 °C eliminates both the α and ϵ phases. Upon cooling, the nanowires do not revert back to the hcp phase, even after several months.

Several researchers have reported pressure-mediated phase transitions at extremely high pressures (>1 kbar), such as the transition of germanium from the diamond

(34) Ram, S. *Acta Mater.* **2001**, *49*, 2297.

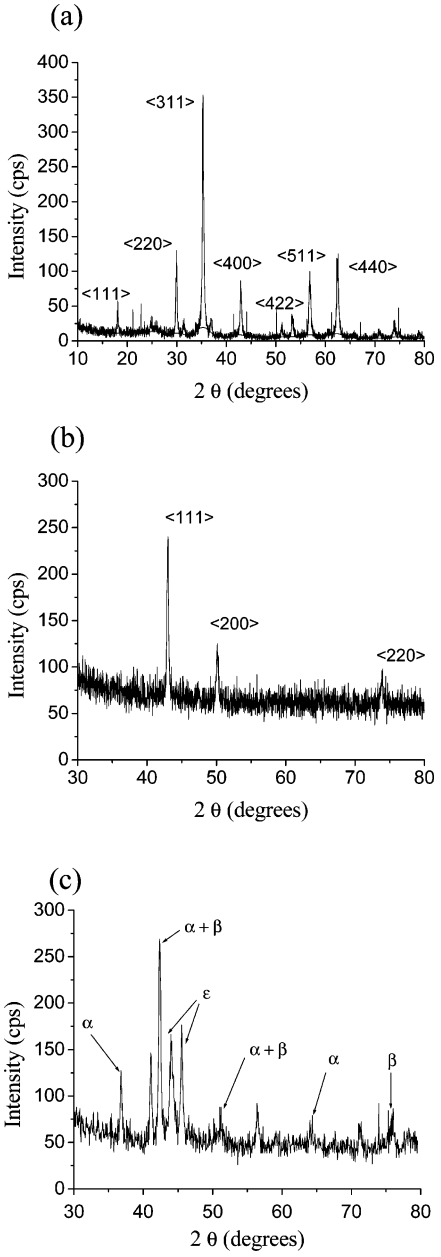

Figure 3. PXRD patterns of mesoporous silica after inclusion of (a) Fe_3O_4, (b) copper, and (c) cobalt.

Table 1. Effect of Reaction Conditions on Cobalt Phase Synthesized

pressure (bar)	temp (°C)	crystal phase (%)			fluid density (g cm^{-3})
		α	*β*	*ϵ*	
138	300	42.9	15.9	41.2	0.132
276	325	5.7	9.0	85.3	0.247
276	350	7.4	15.5	77.1	0.234
276	477	28	31.7	40.3	0.187
276	500	0	100	0	0.180
345	400	76.5	23.5	0	0.261
345	500	0	100	0	0.221

to the denser tetragonal phase.[35] Holmes et al.[36] have shown that pressure can be utilized to control growth direction; however, to our knowledge no one has reported the pressure-sensitive synthesis of different phases at low pressures (250−400 bar). The ability to manipulate the crystal structure of the Co nanowires is of considerable importance due to the strong correlation between the crystal structure and the magnetic properties of bulk Co. The high magnetic coercivity of the hcp phase is the preferred structure for permanent magnetic applications (recording media), while the more symmetric low-coercivity fcc phase is more useful for soft magnetic applications.[4]

Nanotubes of these metals and metal oxides with different thicknesses can be synthesized within the silica mesopores by controlling the precursor concentration. Figure 4 shows a HRTEM image of Fe_3O_4 nanotubes protruding from the surface of mesoporous silica. This mesoporous silica sample (unfilled pore diameter of 7 nm) was loaded with an iron precursor sufficient to only partially fill the mesopores. As seen in Figure 4, nanotubes with a wall thickness of 1.2 nm and an

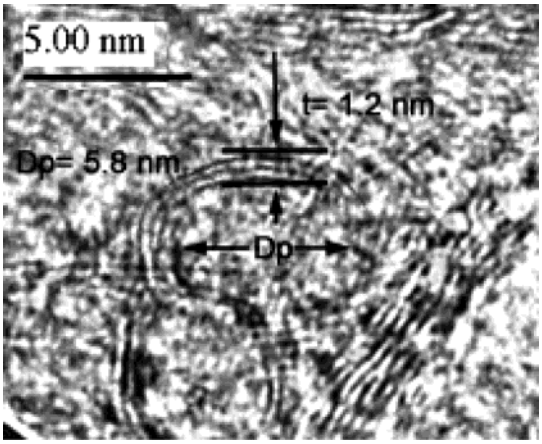

Figure 4. HRTEM image of Fe_3O_4 nanotubes protruding from the surface of mesoporous silica. Synthesized at 450 °C and 345 bar.

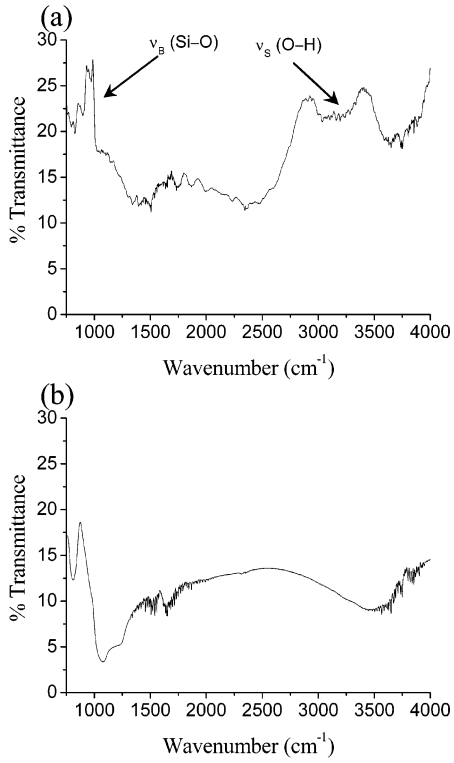

Figure 5. FTIR spectra of (a) calcined mesoporous silica and (b) after partial inclusion of cobalt.

(35) Kasper, J. S.; Richards, S. M. *Acta Crystallogr.* **1964**, *17*, 752.
(36) Holmes, J. D.; Johnston, K. P.; Doty, R. C.; Korgel, B. A. *Science* **2000**, *287*, 1471.

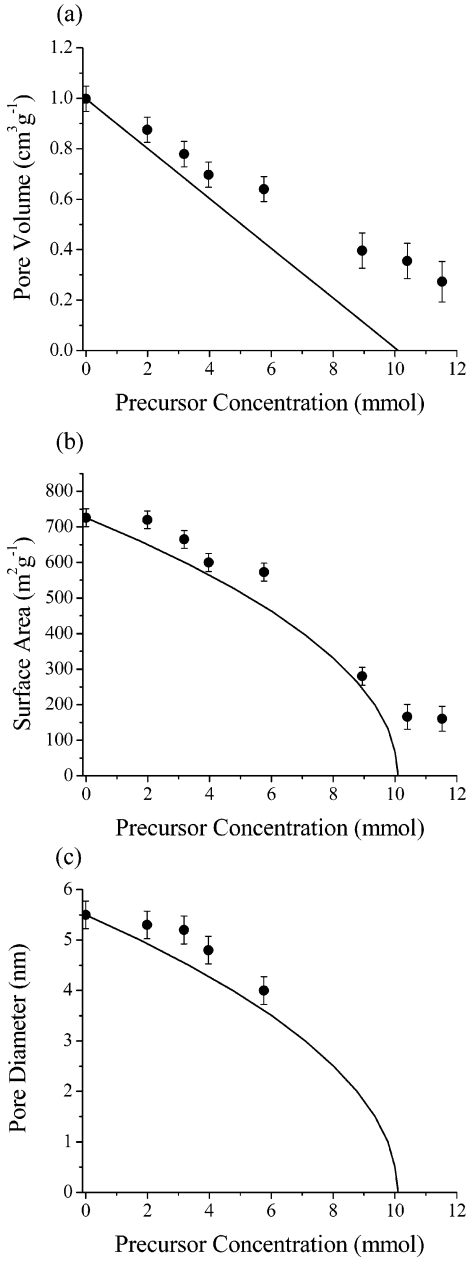

Figure 6. Effect of precursor concentration for Fe_3O_4 on the (a) pore volume, (b) surface area, and (c) pore diameter. The line represents the theoretical changes for nanotube formation.

internal diameter of 5.8 nm were synthesized. N_2 adsorption experiments confirm the presence of nanotubes, suggesting that the pore diameter decreases from 7 nm for the unfilled mesopores to 6.1 nm upon nanotube formation, which is close to the internal diameter of 5.8 nm obtained in the HRTEM image. In addition, FTIR spectroscopy supports the mechanism of nanowire growth through nanotube intermediates. Similar to previous FTIR spectra for completely filled mesopores,[26] the spectra for nanotubes in Figure 5 show decreases in the characteristic silanol vibrational modes at 3700−3200 and 862 cm^{-1} of mesoporous silica, suggesting that the metal atoms are anchored to the walls of the mesopores.

The mechanism of nanowire growth within mesoporous silica was further investigated through nitrogen adsorption measurements. Figure 6 shows how the surface area, pore volume, and pore diameter of the mesoporous silica changed as a function of iron precursor concentration. As seen in Figure 6a,b, the pore volume and surface area decrease with increased amounts of precursor due to the inclusion of the metal into the mesoporous silica. Figure 6c shows the effect of pore diameter as a function of precursor loading. The pore diameter appears to decrease until a diameter of 4 nm. Accurate measurement of pore diameters below 4 nm, however, are difficult because of the limitations of the BJH method at these pore sizes where rapid condensation occurs rather than stepwise layering.[37] If the mechanism of inclusion occurs through nanotube intermediates, the pore volume (V_p) would be expected to decrease as the moles of precursor (n) increase ($V_p \propto n$). However, the pore diameter (d_p) and surface area (SA_p) should decrease nonlinearly ($d_p \propto (1 - n)^{1/2}$, $SA_p \propto (1 - n)^{1/2}$). These calculations are shown in Figure 6 for comparison with the experimental data and suggest that the tubular intermediates, or nanotubes, are a viable mechanism.

Conclusions

We have demonstrated that hexagonal mesoporous silica can serve as template architectures for the production of a range of highly crystalline metallic and metal oxide nanowires and nanotubes. The relatively high diffusion coefficients, higher precursor solubility, and reduced surface tension of high-temperature SCFs result in significant penetrating power and almost complete inclusion of the mesoporous materials with nanowires. When the amount of precursor utilized is controlled, the formation of metal and metal oxide nanotubes can be constructed with various thicknesses. In addition, it was shown that the solution density can be utilized to control the phase synthesized. For example, cobalt can be formed as mixtures of the α, β, and ϵ phases, which can directly affect its magnetic properties.

Acknowledgment. We would like to acknowledge the financial support from Intel (Ireland), Enterprise Ireland for a postdoctoral fellowship to K.J.Z., the Council of Science, and the University of Latvia. The authors would like to thank P. A. Harrington and K. M. Ryan for useful discussions.

CM034139V

(37) Sonwane, C. G.; Bhatia, S. K. *Chem. Eng. Sci.* **1998**, *53*, 3143.